XUV lasing during strong-field-assisted transient absorption in molecules

Timm Bredtmann, Szczepan Chelkowski, André D. Bandrauk, and Misha Ivanov

Phys. Rev. A **93**, 021402 — Published 4 February 2016

DOI: 10.1103/PhysRevA.93.021402

XUV lasing during strong-field assisted transient absorption in molecules

Timm Bredtmann,[1,*] Szczepan Chelkowski,[2] André D. Bandrauk,[2] and Misha Ivanov[1,3]

[1]*Max-Born-Institut, Max-Born-Strasse 2A, D-12489 Berlin, Germany*

[2]*Laboratoire de Chimie Théorique, Faculté des Sciences, Université de Sherbrooke, Sherbrooke, Québec, Canada J1K 2R1*

[3]*Department of Physics, Imperial College London, South Kensington Campus, SW7 2AZ, London, UK*

(Dated: January 14, 2016)

Abstract

Using ab-initio non-Born-Oppenheimer simulations, we demonstrate amplification of XUV radiation in a high-harmonic generation type process using the example of the hydrogen molecular ion. A small fraction of the molecules is pumped to a dissociative excited state from which IR-assisted XUV amplification is observed. We show that starting at sufficiently high IR driving field intensities the ground state molecules become quasi-transparent for XUV radiation, while due to stabilization gain from excited states is maintained. While the basic physics should also be observable in atomic media, the main advantage of the investigated molecular laser is, firstly, efficient lasing from field-free excited states with high mean angular momentum and, secondly, the possibility to tune the amplified XUV frequency windows via control of the internuclear distance.

High-order harmonic generation (HHG) in gases is a table-top technique producing attosecond pulses from the vacuum ultraviolet to the soft x-ray region and beyond [1], opening, in particular, the field of attosecond science [2]. Its challenge, however, is the low conversion efficiency. One option to address this challenge is to rely on phase matching, see e.g. [3–6]. Alternatively, HHG may be enhanced at the single atom/molecule level by enhancing the first step of the HHG process – ionization – seeding it with single attosecond pulses or pulse trains, see e.g. [7–11].

Here, we focus on the recombination step in HHG and explore the possibility of IR-assisted stimulated XUV recombination from excited states, leading ideally to exponential growth of the XUV signal with the particle density, as opposed to quadratic growth in standard HHG (Figure 1(a)). While HHG is a coherent process, it begins as spontaneous: no incident field is originally present at the HHG frequencies to stimulate the emission. As the generated high-frequency light is accumulated in the medium, it may start to stimulate both emission and absorption at these new frequencies. Whether these stimulated transitions would lead to loss or self-seeded XUV light amplification depends on the dynamics of a quantum system. Crucially, the strong IR driving field alters and controls its response, see e.g. [12–17] for some striking examples of what such a control field can achieve.

If an effective population inversion is created between the states during or after the interaction with the strong IR driving field, light emitted at the corresponding transition frequencies can be amplified. Parametric amplification might also be possible, with the energy transferred from the driving field to the XUV field via nonlinear interaction with the medium. This mechanism was suggested [18, 19] as explanation of HHG amplification reported in Ref. [18], see also Ref. [20]. Our ab-initio simulations include both possibilities.

Excitations of excited states during HHG occur e.g. due to frustrated tunnelling [21, 22], via field-induced Freeman resonances [23] or due to the lower harmonics of the IR radiation generated in the medium. It may play an important role during HHG in dense gases. Here, however, we model electronic excitation as a separate step. This choice allows for a systematic analysis of the parameter ranges involved. Likewise, we split the generation of the primary harmonic seed light and its amplification into separate stages. This choice allows us to look at the transient absorption setup, where an XUV probe can be moved relative to the dressing IR driver, leading to amplification of the XUV probe. Moreover such splitting could also help one to exploit the full potential of XUV amplification [24].

Specifically, we consider the molecular medium H_2^+. A short femtosecond pulse (Figure 1(b), blue) excites a nuclear wavepacket from the electronic ground state $\sigma_g 1s$ into the dissociative excited state $\sigma_g 2p$ (Figure 1(c)) via a two-photon transition, with the intermediate state $\sigma_u 1s$. Next, a time-delayed combination of a strong IR driving field (Figure 1(b), black) and a weak XUV probe pulse (red), which stimulates absorption or emission, interacts with both the ground state and the small fraction of excited dissociating molecules. Short duration of the time-delayed probe allows one to think of a transient, time-dependent electronic spectrum for the dissociating molecules.

Figure 1(d) sketches the key absorption and emission channels for the XUV probe pulse (red arrows) with and without the strong IR field (black arrows). In the absence of the IR pulse, XUV absorption is the only channel both for the unexcited (left) and the excited (right) molecules. We show that adding the IR field to the probe XUV attenuates absorption from the unexcited molecules, while IR-assisted XUV stimulated recombination of the excited molecules to lower states leads to amplification of the XUV pulse accompanied by the absorption of many IR photons. The amplified windows in the XUV range depend on the internuclear distance and may be controlled by timing of the pump pulse and the XUV–IR pair.

Two comments are in order: First, the amplifier may operate over a wide tunable spectral range. Second, we find that even if the number of excited molecules is much less than the number of unexcited ones, IR-assisted XUV amplification can still occur, reminding of 'lasing without inversion' (see e.g. [25–29]).

We solve numerically the 3-body, Non-Born-Oppenheimer time-dependent Schrödinger equation for the model molecule H_2^+ (atomic units, a.u., e=$\hbar$=$m_{\rm el}$=1 are used):

$$i\frac{\partial\Psi(z,R,t)}{\partial t} = H(z,R,t)\Psi(z,R,t), \tag{1}$$

where

$$H(z,R,t) = -\beta\frac{\partial^2}{\partial z^2} - \frac{1}{m_{\rm p}}\frac{\partial^2}{\partial R^2} + \frac{1}{R} + V_{\rm C}(z,R) + \kappa z E(t),$$

with

$$\beta = \frac{2m_{\rm p}+m_{\rm e}}{4m_{\rm p}m_{\rm e}}, \qquad \kappa = 1 + \frac{m_{\rm e}}{2m_{\rm p}+m_{\rm e}}$$

and the soft core potential

$$V_{\rm C}(z,R) = \frac{-1}{\sqrt{(z-R/2)^2+1}} + \frac{-1}{\sqrt{(z+R/2)^2+1}},$$

is the three body Hamiltonian after separation of the center-of-mass motion. Both the nuclei and the electron are restricted to one dimension (see e.g. [30]). Here, z is the electron coordinate and R is the internuclear distance.

The electric field for each pulse is defined via the vector potential $A(t)$ [31]. Sine-squared functions are used for the envelopes of the $A(t)$ for each pulse, as in [31, 32]. The carrier envelope phase ϕ for all pulses (as defined in Ref. [31]) is set to $\pi/2$, i.e., a sine pulse is used. The total pulse durations are $T_{\mathrm{IR}} = 5.3\,\mathrm{fs}$ [2.7 fs full width at half maximum (FWHM)] for IR and $T = 2.7\,\mathrm{fs}$ [1 fs full width at half maximum (FWHM)] for both the VUV pump and the XUV seed, Figure 1(b). While intensities of the 800 nm IR driving pulse and of the 134 nm VUV pump pulse are systematically varied, the intensity of the XUV seed with variable central frequency Ω_{XUV} is set to $I_{\mathrm{XUV}} = 5 \times 10^{12}\,\mathrm{W/cm^2}$, which was tested to yield stable numerical results while being in the linear response regime.

The total wavefunction of the system is $\Psi(z, R, t) = \Psi_{\mathrm{IR}}(z, R, t) + \Delta\Psi_{\mathrm{XUV}}(z, R, t)$. Here $\Psi_{\mathrm{IR}}(z, R, t)$ is the wavefunction of the IR dressed system, which also includes the effect of the pump pulse, and $\Delta\Psi_{\mathrm{XUV}}(z, R, t)$ is the perturbation due to the weak XUV probe. The induced dipole moment is

$$\begin{aligned}
&\langle\Psi(t)|\hat{d}|\Psi(t)\rangle = \langle\Psi_{\mathrm{IR}}(t)|\hat{d}|\Psi_{\mathrm{IR}}(t)\rangle \\
&+\langle\Psi_{\mathrm{IR}}(t)|\hat{d}|\Delta\Psi_{\mathrm{XUV}}(t)\rangle + \langle\Delta\Psi_{\mathrm{XUV}}(t)|\hat{d}|\Psi_{\mathrm{IR}}(t)\rangle \\
&+\langle\Delta\Psi_{\mathrm{XUV}}(t)|\hat{d}|\Delta\Psi_{\mathrm{XUV}}(t)\rangle,
\end{aligned}$$

where $\hat{d}$ is the dipole operator. The first term on the right describes the non-linear response to the strong IR field alone, without any assistance from the XUV. Thus, it does not include any XUV stimulated processes and contains only spontaneous HHG-type emission during radiative recombination. The second and third terms describe stimulated emission/absorption of XUV radiation by the IR dressed system, the subject of this paper. The last term depends quadratically on the weak XUV probe field and may thus be neglected for sufficiently low XUV intensities. For increased numerical stability, we use the dipole accelerations $a(t) = -\langle\Psi(t)|\big[H,[H,z]\big]|\Psi(t)\rangle$ and $a_{\mathrm{IR}}(t) = -\langle\Psi_{\mathrm{IR}}(t)|\big[H,[H,z]\big]|\Psi_{\mathrm{IR}}(t)\rangle$. Hence, to identify stimulated absorption and emission of the XUV probe, we calculate the frequency resolved linear response of the IR dressed system to the XUV probe pulse as

$$D_{\mathrm{XUV}}(\Omega) = \frac{1}{\Omega^2}\int dt e^{i\Omega t}(a(t) - a_{\mathrm{IR}}(t)), \tag{2}$$

thereby removing the contribution of the standard HHG-type emission. The numerical propagation is carried out until the end of the XUV probe pulse. The XUV probe absorption/emission is related to the out-of-phase component of $D_{\mathrm{XUV}}(\Omega)$ with respect to the spectral amplitude of the XUV pulse, $E_{\mathrm{XUV}}(\Omega)$. The XUV probe absorption signal is [33]

$$S_{\mathrm{XUV}}(\Omega) \propto \frac{\mathrm{Im}(\mathrm{E}^{*}_{\mathrm{XUV}}(\Omega)\mathrm{D}_{\mathrm{XUV}}(\Omega))}{\int d\Omega |E_{\mathrm{XUV}}(\Omega)|^2}. \tag{3}$$

Figure 2(a) explores the possibility of light amplification from the excited molecules ($\sigma_{\mathrm{g}}2\mathrm{p}$, left) and the reponse of the ground state molecules ($\sigma_{\mathrm{g}}1\mathrm{s}$, right) for a XUV probe-pulse for the intensity range $\mathrm{I_{IR}}$=1×10^{13} W/cm^2 - 9×10^{15} W/cm^2 of the IR driving field for time-delays Δ_{IR}=3 fs and Δ_{XUV}=2.4 fs, c.f. Figure 1(b). The central frequency of the XUV probe is set to $\Omega_{\mathrm{XUV}} = \Omega_{\mathrm{res}} + 7\Omega_{\mathrm{IR}}$=20.4 eV, where Ω_{IR} is the central frequency of the 800 nm IR pulse and Ω_{res}=9.5 eV denotes the resonant transition frequency $|\sigma_{\mathrm{g}}2\mathrm{p}\rangle \rightarrow |\sigma_{\mathrm{u}}1\mathrm{s}\rangle$ for the employed delay-time. First, we assume complete population transfer to the excited state $\sigma_{\mathrm{g}}2\mathrm{p}$ at time zero. While there is only XUV absorption below $\mathrm{I_{IR}}$=5×10^{13} W/cm^2, we identify three regimes for higher IR intensities, see Figure 2(b) which shows the integrated XUV transient absorption spectrum, $\int S_{\mathrm{XUV}}(\Omega)\mathrm{d}\Omega$, both for the excited state (red) and the ground state molecules (blue). For comparison, the corresponding integrated signal strength without the IR driving field is indicated by the horizontal arrows.

In regime (I), strong negative absorption from the excited state molecules yields a first amplification maximum at $\mathrm{I_{IR}}$=1×10^{14} W/cm^2. This gain from the excited state molecules is accompanied by comparable XUV light absorption from the ground state molecules. One can think of an effective mixture of the two molecular species: excited and unexcited, with different electronic spectra [32]. As the excited molecules dissociate (Figure 1(b)), the molecular geometry-dependent spectrum of the electronic transitions changes and an effective population inversion may be created even with the number of excited, dissociating molecules being smaller than the number of unexcited, ground state molecules. However, in regime (I), the comparable absorption from ground state molecules presents a major challenge. In regime (II), rapid IR-induced depletion of the excited state reduces amplification from excited molecules and XUV absorption from the ground state molecules dominates. Starting with intensities $\mathrm{I_{IR}}$=2×10^{15} W/cm^2 (regime (III)), one enters the stabilization regime for the excited states [21, 22, 34–36], resulting in striking XUV light amplification with maximum at $\mathrm{I_{IR}}$=3×10^{15} W/cm^2, being even stronger than in regime (I). At the same time, the ground

state molecules become quasi-transparent due to rapid depletion.

This gain without nominal population inversion is stable over a large range of XUV-probe time-delays Δ_{XUV} (Figure 2(c)) and is maintained for non-overlapping pulses for $\Delta_{\mathrm{XUV}} > 4\,\mathrm{fs}$, c.f. Figure 1(b). Moreover, the gain is stable over a large range of XUV pulse durations (Figure 3), i.e. is robust with respect to possible XUV pulse reshaping during macroscopic light propagation through the molecular medium.

Figure 4 explores, for the full pump-probe scenario, the dependence of the integrated XUV transient absorption signal both on the delay of the IR driving field, Δ_{IR}, and on the central frequency of the XUV seed, Ω_{XUV}. The pump intensity is set to $\mathrm{I_{pump}}{=}3{\times}10^{13}\,\mathrm{W/cm^2}$, exciting 18% of the ground state molecules to electronic state $\sigma_{\mathrm{u}}1\mathrm{s}$ and 16% to the dissociative excited state $\sigma_{\mathrm{g}}2\mathrm{p}$. The remaining parameters are identical to Figs. 2(a)+(b). Even with 83% of the molecules residing in the two lowest electronic states, tunable XUV light amplification is demonstrated. Control of the internuclear distance R through the pump-probe time delay Δ_{IR} allows the effective amplification of XUV pulses with central frequencies Ω_{XUV} ranging from the pump carrier frequency (Ω_{XUV}=9.25 eV) up to at least Ω_{XUV}=22 eV. Importantly, the broad amplification windows centered around Ω_{XUV}=11 eV and Ω_{XUV}=17 eV yield overall gain irrespective of the pump-probe synchronization.

Finally, Figure 4(b) illustrates the strength of the overall gain. In principle, since for the employed IR intensity $\mathrm{I_{IR}}{=}3{\times}10^{15}\,\mathrm{W/cm^2}$ the absorption by the ground state molecules is suppressed (Figure 2(b)), excitations of less than 1% will already yield overall gain. Figure 4(b) determines the pump intensity needed such that the overall gain in the full pump-probe simulations matches the absorption from the unperturbed molecules, i.e. in the absence of both the VUV pump and the IR pulse. The results are indicated by the vertical arrows, black for XUV seeds centered at Ω_{XUV}=15.7 eV for long internuclear distances using delays Δ_{IR} = 14.9 fs, and red for central frequency Ω_{XUV}=18.8 eV for short internuclear distances using Δ_{IR} = 3.9 fs. The corresponding populations after the pump pulse in the state $\sigma_{\mathrm{g}}2\mathrm{p}$ are 8% for Ω_{XUV}=15.7 eV (black) and 15% for Ω_{XUV}=18.8 eV (red).

In conclusion, we have shown that absorption of multiple IR photons from the strong laser field can be accompanied by amplification of weak XUV light incident on the H_2^+ molecule. Amplification is enabled by excitation to a dissociative excited state and controled by molecular dynamics. The XUV absorption from the excited molecules is suppressed in favour of IR-assisted, stimulated XUV recombination into the lower-lying bound states.

Based on the intensity of the IR-driving field, we indentify different gain regimes with distinct physical mechanisms and conversion efficiencies (Figure 2(a)+(b)). In the low intensity regime (I), molecular dissociation makes electronic transition energies time-dependent such that an effective population inversion may be created even when the number of excited, dissociating molecules is smaller than the number of unexcited, ground state molecules. However, in regime (I), absorption from the unexcited molecules presents a major challenge. On the other hand, in the high intensity regime (III) rapid depletion makes the overall response of the ground state molecules quasi-transparent. At the same time, stabilization of excited states yields overall gain even at small degrees of excitation, leading to stronger XUV lasing than in regime (I).

The process takes advantage of the stability of excited electronic states, with the strong-IR-driven wavefunction oscillating as a nearly free Kramers-Henneberger-like quasi-bound wavepacket [34–36]. It is shown that, in regime (III), exciting merely 8%-15% of the molecules suffices already for the overall gain to be equal to the overall absorption by the unperturbed molecules, i.e. in the absence of the pump and the IR pulse (Figure 4(b)). While the basic physics in the high intensity regime (III) should also be observable in atomic media, the main advantage of the investigated molecular laser is, firstly, efficient lasing from field-free excited states with high mean angular momentum (Figure 2(c)) and, secondly, the possibility to tune the amplified XUV frequency windows via control of the internuclear distance (Figure 4(a)). Hence, this amplifier operates over wide spectral windows, controled by the internuclear distance via the pump-probe time delay.

Concerning the synchronization of the pulses, amplification occurs for a range of IR-XUV time-delays of about 3 fs, much longer than the XUV half-cycle. Thus, phase matching carrier oscillations of the XUV-IR pair within one XUV half-cycle is not required. For the pump step, deviations of at least 1 fs are tolerated. Moreover, for specific but broad ranges of central XUV frequencies, overall gain is demonstrated without pump-probe synchronization. Hence, for such frequency windows, the external addition of both the pump pulse and the XUV-seed may become obsolete in dense gases, resulting in self-seeded amplification, with electronic excitations originating either via multi-photon transitions induced by the VUV radiation generated in the medium, or through frustrated tunnelling [21, 22]. We also bring the readers attention to recent papers [37, 38] where high harmonic generation with and without an additional XUV pulse was studied. The key difference in our analysis is that

we explicitly focus on the imaginary part of the system response to the XUV probe, i.e. absorption or gain, while Refs. [37, 38] do not differentiate between real and imaginary parts of the response.

T.B. and M.I. acknowledge partial financial support from US AirForce grant FA9550-12-1-0482. M.I. acknowledges partial support of the EPSRC Programme Grant, and the Marie Curie CORINF network. We thank S. Popruzhenko, O. Smirnova and S. Patchkovskii for stimulating discussions.

* Timm.Bredtmann@mbi-berlin.de

[1] T. Popmintchev, M.-C. Chen, D. Popmintchev, P. Arpin, S. Brown, S. Alisauskas, G. Andriukaitis, T. Balciunas, O. D. Mücke, A. Pugzlys, A. Baltuka, B. Shim, S. E. Schrauth, A. Gaeta, C. Hernández-Garcia, L. Plaja, A. Becker, A. Jaron-Becker, M. M. Murnane, and H. C. Kapteyn, Science **336**, 1287 (2012).

[2] F. Krausz and M. Ivanov, Rev. Mod. Phys. **81**, 163 (2009).

[3] A. Rundquist, C. G. Durfee III, Z. Chang, C. Herne, S. Backus, M. M. Murnane, and H. C. Kapteyn, Science **280**, 1412 (1998).

[4] A. Paul, R. A. Bartels, R. Tobey, H. Green, S. Weiman, I. P. Christov, M. M. Murnane, H. C. Kapteyn, and S. Backus, Nature **421**, 51 (2003).

[5] E. A. Gibson, A. Paul, N. Wagner, R. Tobey, D. Gaudiosi, S. Backus, I. P. Christov, A. Aquila, E. M. Gullikson, D. T. Attwood, M. M. Murnane, and H. C. Kapteyn, Science **302**, 95 (2003).

[6] X. Zhang, A. L. Lytle, T. Popmintchev, X. Zhou, H. C. Kapteyn, M. M. Murnane, and O. Cohen, Nature Physics **3**, 270 (2007).

[7] A. D. Bandrauk and N. H. Shon, Phys. Rev. A **66**, 031401(R) (2002).

[8] E. J. Takahashi, T. Kanai, K. L. Ishikawa, Y. Nabekawa, and K. Midorikawa, Phys. Rev. Lett. **99**, 053904 (2007).

[9] J. Biegert, A. Heinrich, C. P. Hauri, W. Kornelis, P. Schlup, M. P. Anscombe, M. B. Gaarde, K. J. Schafer, and U. Keller, J. Mod. Opt. **53**, 87 (2006).

[10] F. Brizuela, C. M. Heyl, P. Rudawski, D. Kroon, L. Rading, J. M. Dahlstrom, J. Mauritsson, P. Johnsson, C. L. Arnold, and A. L'Huillier, Sci. Rep. **3**, 1410 (2007).

[11] M. Tudorovskaya and M. Lein, J. Mod. Opt. **61**, 845 (2014).

[12] S. E. Harris and A. V. Sokolov, Phys. Rev. Lett. **81**, 2894 (1998).

[13] A. V. Sokolov, D. D. Yavuz, and S. E. Harris, Opt. Lett. **24**, 557 (1999).

[14] A. V. Sokolov, D. R. Walker, D. D. Yavuz, G. Y. Yin, and S. E. Harris, Phys. Rev. Lett. **85**, 562 (2000).

[15] V. A. Polovinkin, Y. V. Radeonychev, and O. Kocharovskaya, Opt. Lett. **36**, 2296 (2011).

[16] V. A. Antonov, Y. V. Radeonychev, and O. Kocharovskaya, Phys. Rev. Lett. **110**, 213903 (2013).

[17] J. Herrmann, M. Weger, R. Locher, M. Sabbar, P. Rivière, U. Saalmann, J.-M. Rost, L. Gallmann, and U. Keller, Phys. Rev. A **88**, 043843 (2013).

[18] J. Seres, E. Seres, D. Hochhaus, B. Ecker, D. Zimmer, V. Bagnoud, T. Kuehl, and C. Spielmann, Nature Phys. **6**, 455 (2010).

[19] J. Seres, E. Seres, and C. Spielmann, Phys. Rev. A **86**, 013822 (2012).

[20] E. A. Nersesov, S. V. Popruzhenko, D. F. Zaretsky, W. Becker, and P. Agostini, Phys. Rev. A **64**, 023419 (2001).

[21] T. Nubbemeyer, K. Gorling, A. Saenz, U. Eichmann, and W. Sandner, Phys. Rev. Lett. **101**, 233001 (2008).

[22] U. Eichmann, A. Saenz, S. Eilzer, T. Nubbemeyer, and W. Sandner, Phys. Rev. Lett. **110**, 203002 (2013).

[23] R. R. Freeman, P. H. Bucksbaum, H. Milchberg, S. Darack, D. Schumacher, and M. E. Geusic, Phys. Rev. Lett. **59**, 1092 (1987).

[24] L. Gallmann, Nature (News and Views) **6**, 406 (2010).

[25] S. E. Harris, Phys. Rev. Lett. **62**, 1033 (1989).

[26] M. O. Scully and M. Fleischhauer, Science **263**, 337 (1994).

[27] O. Kocharovskaya, Physics Reports **219**, 175 (1992).

[28] M. O. Scully and M. S. Zubairy, *Quantum Optics* (Cambridge University Press, 1997).

[29] J. Mompart and R. Corbalán, Journal of Optics B: Quantum and Semiclassical Optics **2**, R7 (2000).

[30] S. Chelkowski, C. Foisy, and A. D. Bandrauk, Phys. Rev. A **57**, 1176 (1998).

[31] A. de Bohan, P. Antoine, D. B. Milošević, and B. Piraux, Phys. Rev. Let. **81**, 1837 (1998).

[32] T. Bredtmann, S. Chelkowski, and A. D. Bandrauk, Phys. Rev. A **84**, 021401 (2011).

[33] S. Mukamel, *Principles of nonlinear optical spectroscopy* (Oxford University Press, 1995).

[34] A. M. Popov, O. V.Tikhonova, and E. A. Volkova, J. Mod. Opt. **58**, 1195 (2011).

[35] F. Morales, M. Richter, S. Patchkovskii, and O. Smirnova, PNAS **108**, 2011 (2011).

[36] M. Richter, S. Patchkovskii, F. Morales, O. Smirnova, and M. Ivanov, New Journal of Physics **15**, 083012 (2013).

[37] C. Serrat, Phys. Rev. Lett. **111**, 133902 (2013).

[38] C. Serrat, D. Roca, and J. Seres, Optics Express **23**, 4867 (2015).

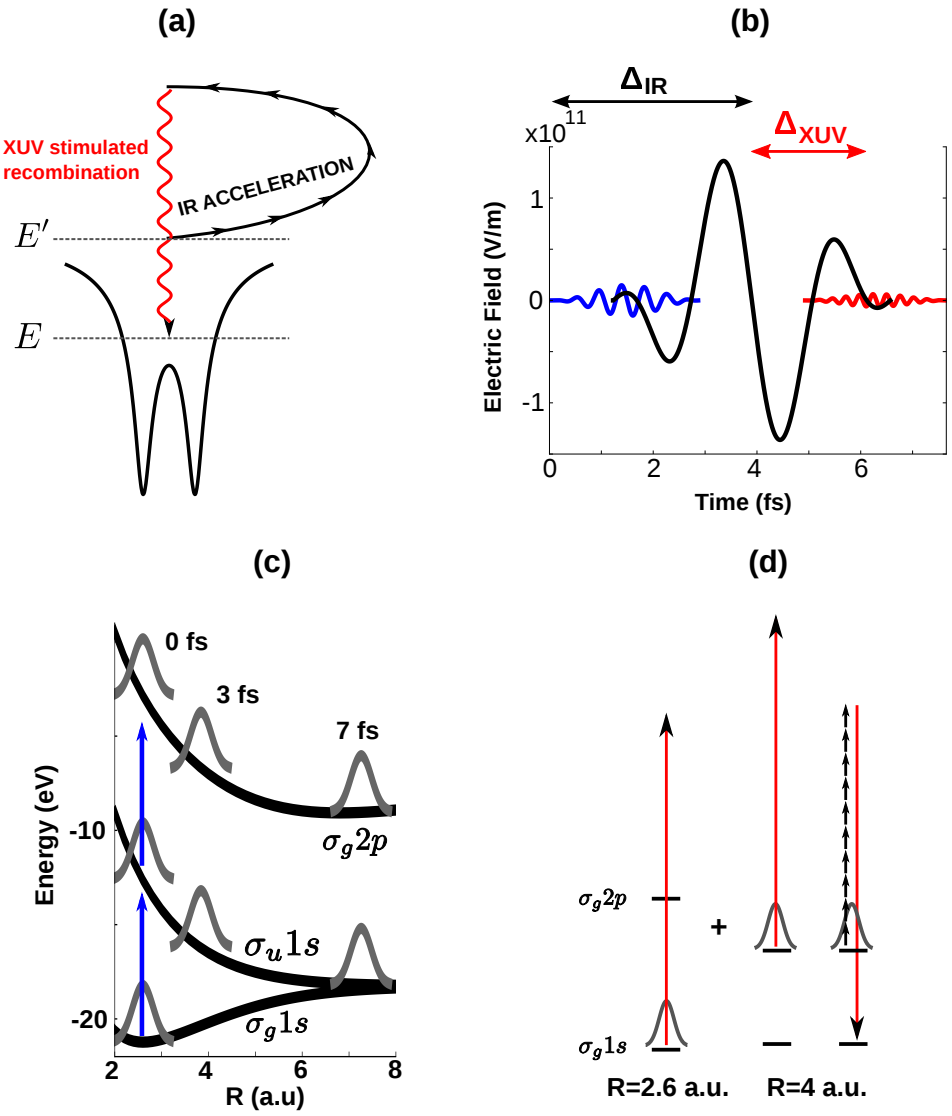

FIG. 1. Schematics of IR-assisted amplification of XUV light in the molecular ion H_2^+. (a) In a HHG-type process, a strong IR pulse drives an electronic excited state. Recombination is stimulated by the weak XUV seed present in the medium. (b) Combination of VUV pump pulse (blue), IR driving field (black) and XUV probe pulse (red) used in the simulations. (c) A fraction of the molecules is pumped via a two photon transition to a dissociative electronic excited state. Timing of the IR driving field allows the control of XUV amplification. (d) In the absence of the IR pulse, XUV absorption (red arrow) is possible both by the unexcited (left, internuclear distance R=2.6 a.u.) and the excited molecules (right, sketched for internuclear distance R=4 a.u.). The intense IR pulse can strongly attenuate XUV absorption while assisting XUV recombination, reminiscent of 'lasing without inversion'.

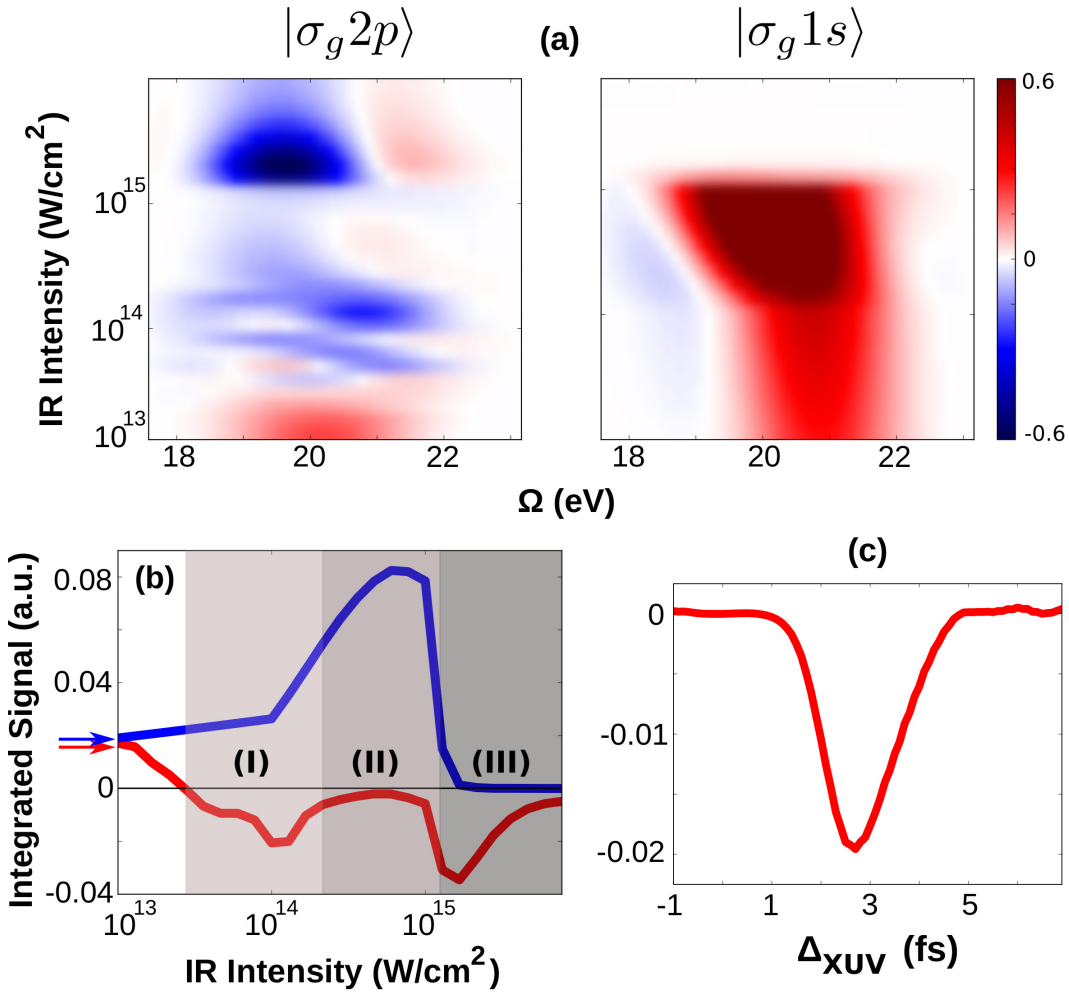

FIG. 2. (a) XUV transient absorption spectra $S_{\mathrm{XUV}}(\Omega)$ from excited state molecules (left) and ground state molecules (right) for variable IR intensities I_{IR} with $\Delta_{\mathrm{IR}} = 3\,\mathrm{fs}$, $\Delta_{\mathrm{XUV}} = 2.4\,\mathrm{fs}$ (c.f. Figure 1(b)) and central XUV frequency Ω_{XUV}=20.4 eV. Here, we assume complete population transfer to the excited state σ_{g}2p at time zero. (b) Corresponding integrated signals, $\int S_{\mathrm{XUV}}(\Omega)\mathrm{d}\Omega$, as function of the intensity of the IR driving field for excited state (red) and ground state (blue) molecules identifying three amplification regimes. Values without the IR pulse are indicated by the horizontal arrows. (c) Dependence of integrated signals from excited state molecules on XUV-probe delay-time for $\mathrm{I_{IR}}$=$5\times10^{15}\,\mathrm{W/cm^2}$.

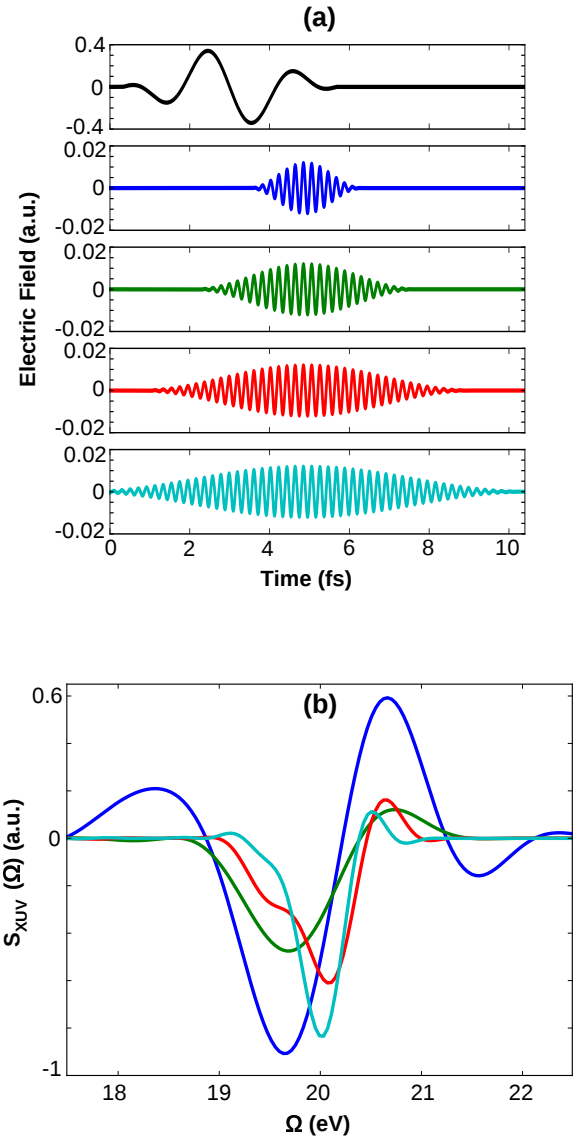

FIG. 3. Influence of the XUV probe pulse duration, T, on the XUV transient absorption spectrum, $S_{\mathrm{XUV}}(\Omega)$, from excited σ_g2p molecules, for $I_{\mathrm{IR}} = 5 \times 10^{15}$ W/cm^2, Δ_{IR}=3 fs, Δ_{XUV} =1.9 fs and Ω_{XUV} =20 eV, c.f. Figure 1(b). (a) From top to bottom: Electric field of the IR and XUV probe pulses with durations $T = 2.75$ (fs) (blue, corresponding to the durations used in the main text), $T = 5.5$ fs (green), $T = 8.25$ fs (red), $T = 11$ fs (cyan). (b) XUV transient absorption spectra, $S_{\mathrm{XUV}}(\Omega)$, for the XUV pulses from (a), shown in corresponding colors.

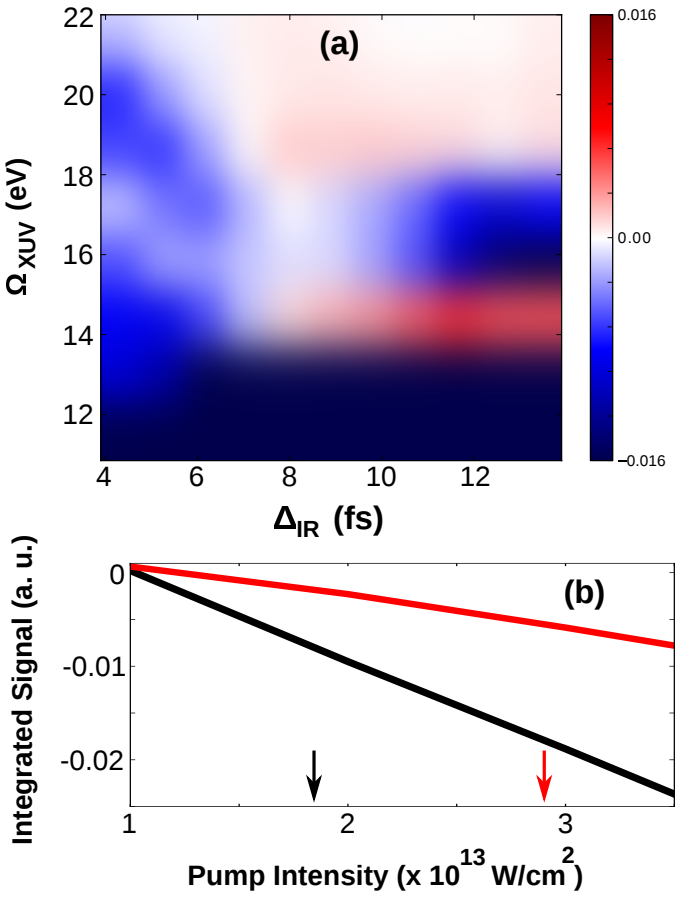

FIG. 4. Full pump-probe simulations: (a) Integrated XUV transient absorption spectrum, $\int S_{\mathrm{XUV}}(\Omega)\mathrm{d}\Omega$, as function of the central frequency of the XUV seed, Ω_{XUV}, and the time delay of the IR driving field, Δ_{IR}. The pump intensity is set to $I_{\mathrm{pump}} = 3\times10^{13}\,\mathrm{W/cm^2}$, exciting 16% of the molecules to the dissociative excited state $\sigma_{\mathrm{g}}2\mathrm{p}$. In all simulations, the intensity of the IR driving field is set to $I_{\mathrm{IR}} = 3\times10^{15}\,\mathrm{W/cm^2}$ and the delay of the XUV seed is Δ_{XUV}=2.4 fs. (b) Integrated signals as function of pump intensity, I_{pump}, with central XUV frequency $\Omega_{\mathrm{XUV}} = 15.7\,\mathrm{eV}$ for large internuclear distances (Δ_{IR}=14.9 fs) (black) and for $\Omega_{\mathrm{XUV}} = 18.8\,\mathrm{eV}$ for short internuclear distances (Δ_{IR}=3.9 fs) (red). The vertical arrows indicate the pump intensities for which the overall gain is equal to the absorption from the unperturbed molecules, i.e. in the absence of the VUV pump and the IR pulse.